Rev. Mexicana Astron. Astrof., **25**, 31-38 (1993)

HIGH FREQUENCY RADIO CONTINUUM OBSERVATIONS OF BARRED SPIRAL GALAXIES

J.A. García-Barreto[1,2], R. Carrillo[1], U.Klein[2,3], and M. Dahlem[4]

Received 1992 October 6

RESUMEN

Hemos observado los flujos de la emisión de radio continuo a 6.3 y 2.8 cm con el radiotelescopio de 100-m en Effelsberg de la región central de un subconjunto de galaxias espirales con barra del catálogo Shapley-Ames. Hemos calculado los índices espectrales para las galaxias detectadas y observamos una correlación entre índices espectrales planos y la temperatura de polvo calculada usando los flujos del *IRAS*, es decir, $T_d \geq 30°$K para galaxias con $\alpha_{20}^{6.3} \geq -0.75$. Los flujos de radio continuo a ambas frecuencias e infrarrojo lejano están fuertemente correlacionados.

ABSTRACT

We have determined the central radio continuum fluxes at 6.3 and 2.8 cm from a subset of barred spiral galaxies from the Shapley Ames Catalog with the 100-m radiotelescope in Effelsberg. We calculated the spectral indices for the galaxies detected and we can see a weak correlation between flat spectral index and dust temperature calculated from *IRAS* fluxes, that is, $T_d \geq 30°$K for galaxies having $\alpha_{20}^{6.3} \geq -0.75$. The radio continuum at both frequencies and the far-infrared fluxes are strongly correlated.

Key words: **GALAXIES-STRUCTRE – RADIO SOURCES-GALAXIES**

1. INTRODUCTION

Previous studies of the radio continuum emission from bright spiral galaxies have revealed that the mean spectral index is $\alpha \simeq -0.75$ independent of the morphology and Hubble type (Klein & Emerson 1981; Gioia, Gregorini, & Klein 1982). Similarly a correlation between the radio continuum emission and the far-infrared emission has been observed in many galaxies (Harwit & Pacini 1975; Helou, Soifer, & Rowan-Robinson 1985). Moreover Hawarden et al. (1986) suggested that higher fluxes of far-infrared emission with radio continuuum from the central regions were found mostly in barred spiral galaxies. Recent high resolution observations of the radio continuum from some barred galaxies like NGC 613, NGC 1097 (Hummel et al. 1987*a*; Hummel, van der Hulst, & Keel 1987*b*), NGC 1326 and NGC 4314 (García-Barreto et al. 1991*a*,*b*) have revealed that there is a central enhancement of star formation in circumnuclear structures also seen in Hα. In order to make a detailed study of the processes that are going on in the central regions of barred spiral galaxies one needs to make high resolution maps of the radio continuum emission as well as broad band and spectroscopy imaging at optical wavelengths.

Our present observations, however, were carried out only to determine the central fluxes of the radio continuum emission and to search for a correlation between far-infrared colors indicative

TABLE 1

TELESCOPE AND RECEIVER PARAMETERS

Parameter	Value	
Frequency (GHz)	4.75	10.7
Bandwidth (MHz)	500	500
Tsys (°K)	66	80
Tb/S (mK/mJy)	2.43	1.88
HPBW (arcmin)	2.44	1.18

[1] Instituto de Astronomía, Universidad Nacional Autónoma de México.

[2] Max Planck Institut für Radioastronomie.

[3] Radio Astronomisches Institut der Universitaet Bonn.

[4] Hamburger Sternwarte.

of star formation with flat spectral indices. For this purpose we observed a subset of barred spiral galaxies from the Shapley Ames catalog at the wavelengths of 6.3 cm and 2.8 cm. These galaxies had been detected at 20 cm by Condon (1987) with the VLA.

2. OBSERVATIONS

We have carried out radio continuum observations of the barred spiral galaxies with the 100-m telescope in Effelsberg in March 1991 at 6.3 cm (4.75 GHz) and 2.8 cm (10.55 GHz). The telescope and receiver parameters are listed in Table 1. The receiver at 2.8 cm was a two-channel, cooled parametric amplifier equipped with two horns with a separation on the sky of 4.88′. The 2.8 cm observations were performed by scanning in right ascension and declination with a scan width of 10′. There were between 10 to 30 subscans in each direction for each source and they were then averaged. The measurements at 6.3 cm have been carried out with a 3-channel cooled system in which the signals from two horns are fed into a hybrid to yield the sum and the difference of the volt-

TABLE 2

GALAXY LIST

Source	Type	(1950.0) R.A. h m s	Dec ° ′ ″	D25	Vhel (km s^{-1})	i °	D Mpc	Tully's Group
n2336	SBbc(r)	07 18 28.0	80 16 35.0	5.7	2196	59	33.9	42–17+16
n2366	SBmIV–V	07 23 34.2	69 18 42.0	8.0	102	70	2.9	14–10
n2835	SBc(rs)	09 15 36.6	–22 08 45.0	6.8	890	48	10.8	54–3+1
n2935	SBb(s)	09 34 26.3	–20 54 12.0	5.4	2275	49	30.6	31–12
n3319	SBc(s)II	10 36 15.2	41 56 56.0	6.7	743	57	11.5	15+7
n3351	SBb(r)II	10 41 19.6	11 58 00.0	7.5	783	56	8.1	15–1
n3359	SBc(s)I	10 43 21.1	63 29 11.0	7.1	1013	55	19.2	12–0+1
n3513	SBc(s)II	11 01 19.2	–22 58 28.0	3.2	1195	38	17.0	54–5
n3686	SBc(s)I	11 25 07.3	17 29 56.0	2.9	1168	42	23.5	21–1
n3729	SB(ring)pec	11 31 05.3	53 24 11.0	3.2	1035	47	17.0	12–1
n3953	SBbc(r)I	11 51 12.9	52 36 20.0	5.9	1054	61	17.0	12–1
n3992	SBb(rs)	11 55 01.0	53 39 13.0	7.4	1051	59	17.0	12–1
n4123	SBbc(rs)	12 05 37.5	03 09 30.0	4.6	1339	39	25.3	22–11
n4214	SBmIII	12 13 08.0	36 36 19.0	9.6	288	37	3.5	14–7
n4236	SBdIV	12 14 21.8	69 44 36.0	19.6	2	73	2.2	14+10
n4242	SBdIII	12 15 01.3	45 54 00.0	5.2	516	50	7.5	14–4
n4487	SBc(s)	12 28 29.2	–07 46 41.0	3.9	1037	49	19.9	11–14+10
n4496	SBcIII	12 29 05.8	04 12 56.0	3.7	1738	43	13.1	11–4+1
n4535	SBc(s)	12 31 47.9	08 28 25.0	6.7	1966	50	16.8	11–1
n4618[a]	SBbc(rs)	12 39 09.5	41 25 29.0	4.2	546	41	7.3	14–4
n4654	SBc(rs)	12 41 25.7	13 23 58.0	4.8	1044	59	16.8	11–1
n4691	SBbpec	12 45 39.5	–03 03 28.8	3.5	1119	32	22.5	11–0+10
n4725	SBb(r)	12 47 59.9	25 46 20.0	10.5	1207	43	12.4	14–2+1
n4902	SBb(s)	12 58 21.3	–14 14 41.0	2.6	2724	17	39.2	11–30
n4981	SBbc(sr)	13 06 13.0	–06 30 48.0	2.8	1677	49	27.8	11–17+10
n5068	SBc(s)	13 16 12.4	–20 46 35.0	7.6	679	29	6.7	14+17
n5236	SBc(s)	13 34 10.2	–29 36 49.0	11.5	518	24	4.7	14–15
n5669	SBc(r)	14 30 17.1	10 06 37.0	4.2	1371	45	24.9	41–0+1
n5792	SBb(s)	14 55 48.2	–00 53 26.0	7.2	1930	81	30.6	41+2+1
n5850	SBb(sr)	15 04 35.5	01 44 17.0	4.6	2530	28	28.5	41–1
n5921	SBbc(s)	15 19 27.2	05 14 53.0	4.9	1480	32	25.2	41–0+1
n6217	RSBbc(s)	16 35 05.1	78 18 05.0	3.5	1359	45	23.9	44–0+5
n6907	SBbc(s)	20 22 07.7	–24 58 18.0	3.4	3155	30	42.1	...
n7479	SBbc(s)	23 02 26.8	12 03 06.0	3.9	2382	45	32.4	64–2+1
n7640	SBc(s)	23 19 42.6	40 34 16.0	9.6	369	85	8.6	65–4
n7723	SBb(rs)	23 36 21.3	–13 14 13.0	3.9	1860	57	23.7	63–6
n7741	SBc(c)	23 41 22.7	25 47 53.0	4.1	750	51	12.3	65–3

From Tully (1988). Throughout this paper H_0 = 75 km/Mpc.
[a] Interacting galaxy? Keel et al. 1985.

ges. The 6.3 cm observations were performed by anning in right ascension and declination with scan width of 15′. There were between 10 30 subscans in each direction centered on the dio position given by Condon (1987) for each urce and they were then averaged. The final ns were about 1.5 mJy/beam area at 6.3 cm and mJy/beam area at 2.8 cm. The point sources 2286, 3C279, NRAO530 and 3C123 have been ed as calibrators with the flux density scale of Baars, Genzel, & Paulini-Toth (1977). A detailed explanation of the equipment and data reduction techniques is found in Klein & Emerson (1981). The peak flux was determined from a Gaussian fit of the averaged subscans. Some of the galaxies were observed to be extended but due to confusion with other sources we preferred to give the peak flux under the beam area and not the corrected flux using the deconvolved size.

TABLE 3

GALAXIES' FIR AND BLUE LUMINOSITIES

Source	*IRAS* Fluxes (Jy)				FIR	Log B	SFR1[a]	SFR2[b]	T_d[c]
	12μm	25μm	60μm	100μm	(10^{-13})		(10^{-3})		°K
n2336	.25L	.25L	0.97	8.96	1.44	10.99	0.400	7.82	22
n2366	.25L	.72L	3.30	4.58	1.65	8.87	0.003	0.06	49
n2835	.25L	.25L	2.56	14.40	2.65	10.06	0.078	0.92	25
n2935	.25L	.41	3.78	12.04	2.74	10.89	0.640	6.21	30
n3319	.25L	.34L	0.69L	2.67	0.56	9.68	0.018	0.39	28
n3351	.57	1.91	17.37	35.30	10.10	9.90	0.167	0.63	35
n3359	.25L	.21	4.06	14.32	3.12	10.43	0.290	2.15	29
n3513	.25L	25L	2.63	7.63	1.82	9.98	0.133	0.76	31
n3686	.31L	.40L	3.45	11.72	2.60	10.17	0.363	1.18	29
n3729	.29L	.37	2.66	7.76	1.84	9.89	0.134	0.62	30
n3953	.25L	.25L	2.86	19.52	3.39	10.44	0.247	2.20	25
n3992	.30L	.25L	.63	9.37	1.38	10.49	0.101	2.47	20
n4123	.40L	1.21	5.98	10.96	3.32	10.29	0.537	1.56	36
n4214	.39	1.75	14.47	25.47	7.91	9.22	0.024	0.13	37
n4236	.25L	0.16	1.60	4.11	1.04	9.10	0.001	0.10	32
n4242	...	...	...	...	...	9.36	...	0.18	...
n4487	.25L	.72L	1.73	7.28	1.48	10.27	0.148	1.49	27
n4496	.25L	.77L	3.59	9.96	2.42	9.80	0.105	0.50	31
n4535	.25L	.69L	6.54	21.48	4.83	10.43	0.344	2.15	30
n4618	.25L	.25L	3.27	11.65	2.53	9.44	0.034	0.22	28
n4654	.86	1.31	13.16	35.26	8.72	10.32	0.621	1.67	32
n4691	.71	2.43	15.18	21.69	7.67	10.24	0.980	1.39	40
n4725	.25L	.25L	.88	7.75L	1.26	10.45	0.049	2.22	23
n4902	.39L	.29L	3.16	12.09	2.55	10.65	0.989	3.57	28
n4981	.29L	.85L	3.59	10.68	2.51	10.36	0.490	1.83	30
n5068	.30L	.95L	2.34	17.12	2.92	9.76	0.033	0.46	24
n5669	.25L	.25L	1.65	5.54	1.23	10.14	0.193	1.10	29
n5792	.84	.94	9.03	19.30	5.37	10.52	1.270	2.65	34
n5850	.25L	.25L	.73	4.43	0.79	10.47	0.162	2.36	25
n5921	.25L	.25L	2.65	10.45	2.18	10.46	0.350	2.30	28
n6217	.48	1.54	10.51	21.14	6.08	10.27	0.877	1.49	35
n6907	.63	1.27	13.36	30.33	8.16	10.46	3.650	2.31	33
n7479	.75	3.32	12.12	24.93	7.08	10.64	1.880	3.49	35
n7640	.25L	.25L	1.71	7.57	1.51	9.98	0.028	0.76	27
n7723	.37L	.46	4.19	10.78	2.72	10.31	0.386	1.63	32
n7741	1.38L	.37L	2.02	7.29	1.57	9.70	0.060	0.40	28

[a] SFR1 is calculated using SFR = 8×10^{-11} L(FIR)/L$_\odot$ $M_\odot$/yr. (Scoville & Young 1983).

[b] SFR2 is calculated using SFR = 8×10^{-11} [L(FIR) + L(Blue)]/L$_\odot$ M$_\odot$/yr. (Scoville & Young 1983).

[c] T_d is the dust temperature using the 60 and 100 μm fluxes and assuming $S_\nu \sim \nu B_\nu(T_d)$. An L after a flux donotes an upper limit.

TABLE 4

GALAXIES' RADIO CONTINUUM[a]

Source	Flux[b]	Expected Flux[c]		Observed Flux					
				6.3 cm			2.8 cm		
	20 cm	6.3 cm	2.8 cm	Flux	Error	rms	Flux	Error	rms
n2336	17.7	7.0	3.6	5.5	0.9	1.2	...	...	...
n2366	25	9.9	5.2	10.7	0.8	1.0	5.9	1.1	0.9
n2835	18.2	7.2	3.7	11.8	1.5	2.5	5.8	1.1	1.2
n2935	40	15.8	8.3	18.9	2.7	3.7	4.8	1.0	1.2
n3351	47.8	18.9	9.9	30.4	1.6	2.5	14.0	1.5	1.5
n3359	50.1	19.8	10.3	14.9	0.9	1.1	3.3	1.0	1.1
n3513	16.1	6.4	3.3	9.2	1.3	1.9	...	...	...
n3686	15.4	6.1	3.2	6.6	1.2	1.8	4.3	0.8	0.5
n3729	20.6	8.1	4.2	9.6	1.9	1.6	4.8	1.6	1.3
n3953	41.1	16.2	8.5	9.5	0.8	1.1	3.2	0.9	1.1
n3992	21.3	8.4	4.4	8.9	1.4	2.3	7.0	0.7	0.8
n4123	22.0	8.7	4.5	11.8	1.7	2.6	8.6	1.0	1.5
n4214	51.9	20.5	10.7	32.5	1.6	2.3	15.8	1.3	1.1
n4236	28.1	11.1	5.8	8.5	0.8	1.0	8.9	1.2	1.4
n4487	1.9	0.7	0.3	8.0	0.7	0.8	2.5	0.8	0.6
n4496	21.1	8.3	4.3	10.4	0.9	1.1	...	...	...
n4535	64.5	25.5	13.3	20.4	0.9	1.3	2.9	0.6	0.7
n4618	31.9	12.6	6.6	13.4	0.8	1.0	4.5	0.9	0.6
n4654	117	46.3	24.2	37.6	2.3	4.3	11.2	0.5	0.6
n4691	47.5	18.8	9.8	27.7	1.2	1.4	16.4	0.4	0.4
n4902	52	20.6	10.7	18.8	0.9	1.1	...	...	...
n4981	21	8.3	4.3	13.2	1.5	2.4	...	...	...
n5068	39	15.4	8.0	10.3	1.6	1.1	...	...	...
n5669	10.7	4.2	2.2	7.3	2.0	2.0	...	...	...
n5792	51.8	20.5	10.7	29.6	1.6	2.5	14.3	0.8	0.8
n5850	17.9	7.1	3.7	8.6	1.8	2.0	...	...	...
n5921	23.1	9.1	4.8	9.4	3.0	2.0	...	...	...
n6217	78.4	31.0	16.2	40.6	0.9	1.5	17.5	1.0	0.9
n6907	136	53.8	28.1	58.8	3.2	6.0	...	...	...
n7479	109	43.1	22.5	45.7	2.2	2.9	13.4	0.6	0.6
n7640	29.3	11.6	6.1	12.1	1.6	2.2	5.0	1.1	0.9
n7741	13.3	5.3	2.7	...	...	...	6.7	0.4	0.4

[a] All fluxes in mJy.

[b] Fluxes at 20 cm are from Condon (1987)

[c] Expected fluxes at 6 cm and 2.8 cm are computed assuming a single non thermal spectral index of −0.8 from 20 cm to 2.8 cm.

TABLE 5

GALAXIES' SPECTRAL INDEX

Source	Spectral Index			Source	Spectral Index			Source	Spectral Index		
	$\alpha_{20}^{6.3}$	$\alpha_{20}^{2.8}$	$\alpha_{6.3}^{2.8}$		$\alpha_{20}^{6.3}$	$\alpha_{20}^{2.8}$	$\alpha_{6.3}^{2.8}$		$\alpha_{20}^{6.3}$	$\alpha_{20}^{2.8}$	c
n2336	−1.0	...	...	n4123	−0.53	−0.48	−0.39	n5068	−1.14	...	
n2366	−0.73	−0.73	−0.74	n4214	−0.40	−0.61	−0.90	n5669	−0.33	...	
n2835	−0.37	−0.58	−0.89	n4236	−1.03	−0.58	+0.05	n5792	−0.48	−0.66	−
n2935	−0.64	−1.08	−1.71	n4487	+1.23	+0.14	−1.43	n5850	−0.63	...	
n3351	−0.39	−0.62	−0.97	n4496	−0.61	...	...	n5921	−0.77	...	
n3359	−1.04	−1.39	−1.88	n4535	−0.99	−1.58	−2.44	n6217	−0.57	−0.76	−
n3513	−0.48	...	...	n4618	−0.74	−1.00	−1.36	n6907	−0.72	...	
n3686	−0.73	−0.65	−0.53	n4654	−0.97	−1.20	−1.52	n7479	−0.75	−1.07	−
n3729	−0.66	−0.74	−0.86	n4691	−0.46	−0.54	−0.65	n7640	−0.76	−0.90	−
n3953	−1.26	−1.30	−1.36	n4902	−0.87	...	...	n7741	...	−0.35	
n3992	−0.75	−0.57	−0.30	n4981	−0.40	...	...				

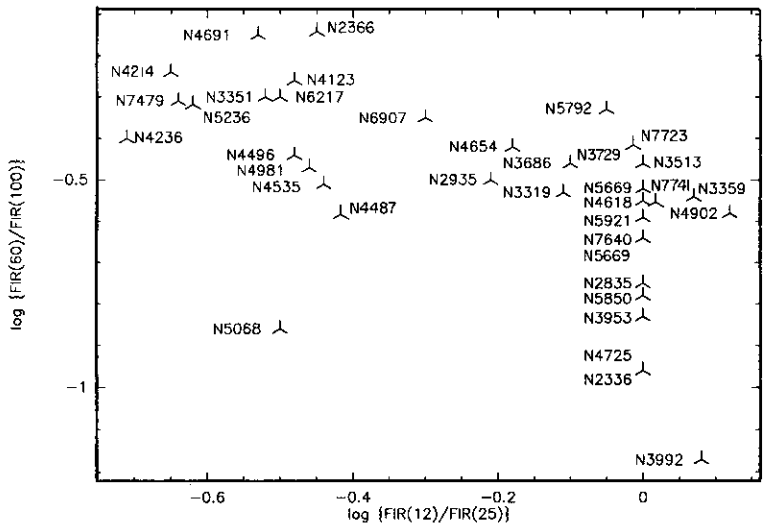

1. Color-color plot of the *IRAS* fluxes of the bright barred galaxies observed. The band from lower right to upper indicates greater current star formation (Helou 1986).

3. RESULTS AND DISCUSSION

Table 2 lists the general characteristics of the erved barred spiral galaxies with coordinates, diameters, heliocentric velocity, inclination with respect to the plane of the sky, distance and group to which the galaxy is a member of. Table 3 lists the *IRAS* fluxes at each wavelength taken from the *IRAS* Point Source Catolog (1988), it lists also the combined far-infrared flux, the blue luminosities and the global star formation rates according to Scoville & Young (1983). Table 4 lists the observed fluxes at 20 cm by Condon (1987), the expected fluxes at 6.3 and 2.8 cm assuming a single spectral index $\alpha = -0.8$ from 20 to 2.8 cm and also the observed fluxes at 6.3 and 2.8 cm using the 100-m radiotelescope. Table 5 gives the derived non-thermal spectral indices using also the fluxes reported by Condon (1987) where we assume $S_\nu \simeq \nu^\alpha$, where S is the flux, ν is the frequency and α is the non-thermal spectral index.

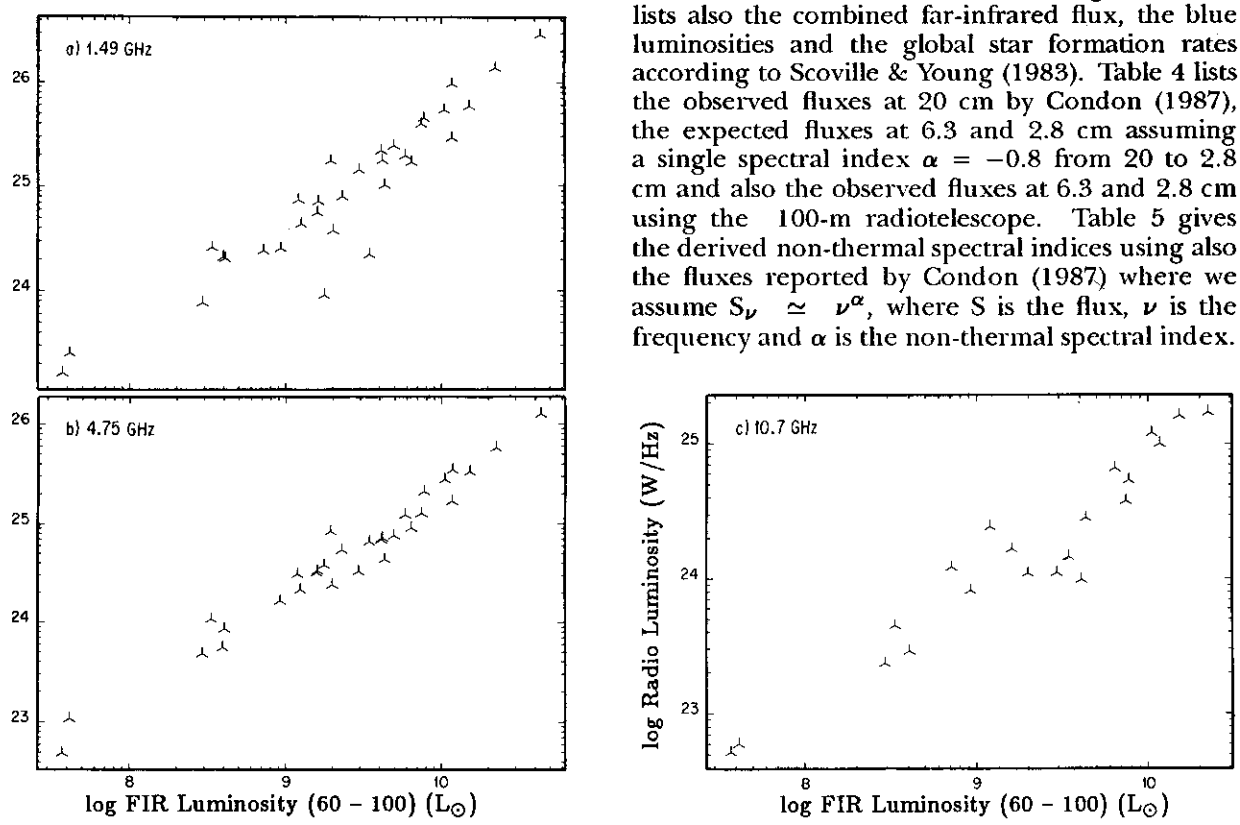

2. Radio luminosity versus *IRAS* far-infrared luminosity for the bright barred galaxies studied here. Note the tight elation between the two bands at every radio wavelength, *a*) 20 cm fluxes from Condon 1987; *b*) 6.3 cm fluxes, this k; *c*) 2.8 cm fluxes, this work.

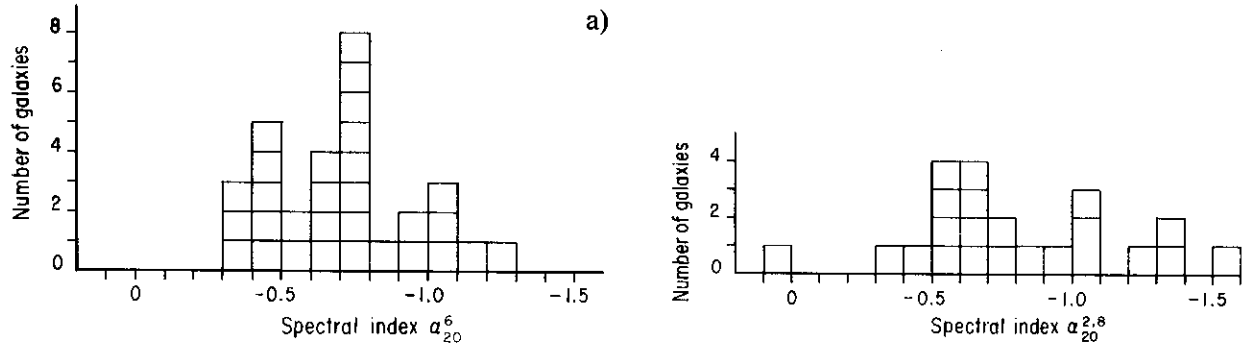

Fig. 3. Number of galaxies versus spectral index: *a*) between 20 and 6.3 cm; *b*) between 20 and 2.8 cm. Notice tha both diagrams about half of the total of galaxies have flatter spectral index than $\alpha = -0.7$.

Figure 1 shows a color-color diagram of the far-infrared (*IRAS*) fluxes of the barred spiral galaxies studied in this paper after Helou (1986). Note that colors lying on the band from lower right to upper left are believed to indicate greater star formation activity (Helou 1986); that is, the dust is heated by the *UV* photons of the newly formated stars and re-radiate in the infrared. Figure 2 shows the radio luminosity versus the far-infrared luminosity at the three observed frequencies. Note that there exists a strong correlation between the radio continuum and the far-infrared at every frequency. This correlation has been observed to hold in other galaxies (Helou et al. 1985) but we believe that this is a global correlation and it is not clear at this moment to us what is the tailed explanation in the context of central s formation activity, due to angular resolution in infrared and radio continuum observations.

We have done the following analysis. First have computed the expected fluxes at 4.7 a 10.7 GHz using the 1.4 GHz fluxes reported Condon (1987) and a constant spectral index of = −0.8 from 1.4 GHz to 10.7 GHz which is a ical spectral index for the emission of spiral ga xies. Second we have compared these expec fluxes with the observed fluxes. 23 out of 32 g axies have higher observed fluxes than expec at 6.3 cm, while 14 out of 32 have higher served fluxes than expected at 2.8 cm; 12 out

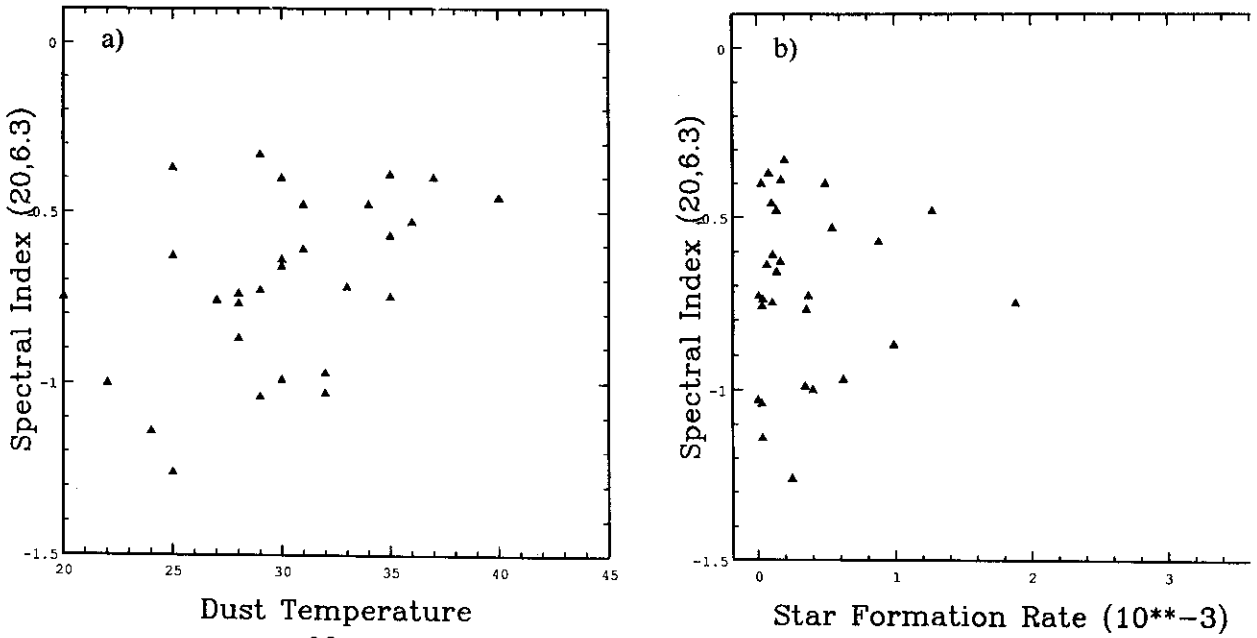

Fig. 4. *a*) Spectral index $\alpha_{20}^{6.3}$ versus dust temperature computed from *IRAS* 60μm and 100μm fluxes. Note that galaxies with $T_d \geq 30°$K have $\alpha_{20}^{6.3} > -0.75$ except for NGC 4236, NGC 4535 and NGC 4654 and are of late Hub type. *b*) Spectral index $\alpha_{20}^{6.3}$ versus star formation rate as listed in Table 3 and calculated using the FIR luminosi according to Scoville & Young (1983).

TABLE 6

HYDROGEN ATOMIC AND MOLECULAR MASSES AND Hα FLUXES

Galaxy	Type	M_T (10^{11} $M_\odot$)	M(H I)[g] (10^9 $M_\odot$)	ΔV_{HI}	$M(H_2)$ (10^8 $M_\odot$)	F(Hα) Total (10^{-13} erg cm^{-2} s^{-1})	F(Hα) Central (10^{-13} erg cm^{-2} s^{-1})	Hα Structure[a]	Scale (pc/arcsec)
2336	SBbc(r)I	4.90	9.48	461	...	31.6[e]	...	...	164.35
2366	SBmIV	0.03	0.8	116	...	...	...	...	14.06
2835	SBc(rs)	0.53	1.1	213	...	...	...	...	52.36
2935	SBb(s)	2.46	4.9	312	...	...	...	...	148.35
3351	SBb(r)II	0.65	0.6	289	7[f]	45.7[d]	3.02[i]	ring	39.27
3359	SBc(s)I	1.22	5	263	0.25[c]	...	...	...	93.08
3513	SBc(s)II	0.16	1.1	112	...	...	...	...	82.41
3686	SBbc(s)I	0.57	0.6	207	...	...	...	...	113.93
3729	SB(ring)pec	2.01	0.5	476	...	...	...	...	82.41
3953	SBbc(r)I	2.05	3.3	424	...	...	...	...	82.41
3992	SBb(rs)	3.38	3.7	476	...	...	...	...	82.41
4123	SBbc(rs)	1.27	3.2	223	...	...	3.46[i]	point like	122.66
4214	SBmIII	0.06	2.4	88	1[h]	144.5[d]	...	...	16.96
4236	SBd IV	0.15	1.5	194	...	...	...	...	10.66
4487	SBc(s)	0.62	1.6	228	...	13.5[d]	...	...	96.47
4496	SBIII	0.30	4.81	182	...	20.4[d]	...	...	63.51
4535	SBc(s)	1.10	5.5	290	69.10[b]	37.2[d]	1.62[i]	point like	81.44
4618	SBbc(rs)	0.15	4.7	157	...	...	0.49[b]	...	35.39
4654	SBc(rs)	0.90	3.4	307	32.10[b]	28.2[d]	0.89[b]	amorphous	81.44
4691	SBbpec	0.54	0.5	149	...	...	5.75[i]	...	109.08
4902	SB(s)	7.69	9.4	272	...	...	0.12[i]	...	190.05
4981	SBbc(sr)	0.91	2.2	276	...	...	...	...	134.78
5068	SBc(s)	0.24	4.2	112	...	...	...	...	32.48
5669	SBc(r)	0.86	2.6	217	...	...	...	...	120.72
5792	SBb(s)	4.33	7.6	469	...	...	...	...	148.35
5850	SBb(rs)	2.44	2.1	217	...	...	0.17[i]	...	138.17
5921	SBbc(s)	1.40	6.3	191	0.78[c]	...	0.17[i]	...	122.17
6217	RSBbc(s)	1.00	5.8	262	3.10	25.7[d]	...	...	115.87
6907	SBbc(s)	6.83	19.7	370	...	...	...	...	204.11
7479	SBbc(s)	3.08	5.7	374	210[j]	13.8[d]	0.52[i]	...	157.08
7640	SBc(s)	0.49	4.3	261	0.07[c]	...	...	...	41.69
7741	SBc(s)	0.33	7.6	214	0.07[c]	19.5[d]	1.07[i]	...	59.63

[a] Pogge 1989; [b] Kenney & Young 1989; [c] Braine & Combes 1992; [d] Kennicutt & Kent 1983; [e] Romanishin 1990; [f] Devereux, Kenney, & Young 1992; [g] Huchtmeier & Richter 1989; [h] Thronson et al. 1988; [i] Keel 1983; [j] Young et al. 1986.

have higher observed fluxes at both frequen- than the fluxes expected with a single spec- index. The relevance of not having a sin- spectral index from 1.4 GHz to 10.7 GHz is the spectrum flattens at higher frequencies. s result is in accordance with previous studies ormal spiral galaxies, that is, the radio conti- m spectrum flattens at frequencies higher than Hz (Giogia et al. 1982; Israel & van der Hulst 3). Figure 3 shows the number of galaxies us spectral index between 1.4 and 10.7 GHz with a clear maximum of 8 galaxies with α between -0.7 and -0.5 and the number of galaxies versus spectral index between 1.4 and 4.75 GHz with 14 galaxies with α less than -0.7. Since we are observing extended sources, most likely a collection of discrete sources on the disk of the galaxies, a flat spectrum suggests a higher thermal origin of the emission due to recent star formation activity. We note a correlation between flat spectral index and warm dust temperature in the sense that all galaxies except NGC 4236, NGC 4535 and

NGC 4654 have $\alpha_{20}^{6.3} > -0.75$ and $T_d \geq 30$°K, as seen in Figure 4, which is in agreement with the results Xu et al. (1992) and Bicay & Helou (1990) have found, namely, that both the warm far infrared ($T_d \geq 30$ K) and the thermal radio emission are associated with young ionizing stars. Persson & Helou (1987) have found, similarly, a strong correlation between the Hα fluxes (and indirectly the thermal radio continuum) and the warm far infrared from the disks of normal spiral galaxies indicating that both emissions originate from young OB stars. Note that there is no clear correlation, however, between flat spectral index $\alpha_{20}^{6.3} > -0.75$ and star formation rate (see Figure 4*b*). Table 6 lists the hydrogen atomic and molecular masses as well as the H_α fluxes. Is there an enhancement of star formation in the central regions, in the bar or on the normal spiral arms of these barred galaxies? We cannot give a proper answer to this question until high angular resolution observations are carried out for each of the galaxies in this study. However by analogy with other barred galaxies that present central activity like NGC 3351 (Devereux, Kenney, & Young 1992); NGC 1097 (Hummel et al. 1987*b*); NGC 1326 and NGC 4314 (García-Barreto et al. 1991*a*,*b*) we believe that it is indeed in the central regions where enhanced star formation activity is taking place (see also Hummel et al. 1990).

4. CONCLUSIONS

We have made 4.75 and 10.7 GHz radio continuum observations of a set of barred spiral galaxies with the 100-m Effelsberg telescope. Our main result is that about half of the number of galaxies observed present a flatter spectral index between 1.4 and 10.7 GHz than the average spectral index, $\alpha = -0.70$, characteristic of the disk emission from spiral galaxies. This result suggest a thermal emission from processes of recent star formation in addition to synchrotron radio continuum emission. A strong correlation of radio continuum and far infrared emissions is observed at every frequency.

We thank the staff of the 100-m Efflesberg telescope for their help during the observations.

J.A.G.-B. acknowledges a Junior Fellowship from the Alexander von Humboldt-Stiftung, Federal Republic of Germany during his stay at the MPIfR. We also thank our secretarial staff of the IA-UNAM their careful typing of the manuscript and A. Gar for drawing the figures.

REFERENCES

Baars, J.W.M., Genzel, R., Pauliny-Toth, I.I.K., & Wit A. 1977, A&A, 61, 99
Bicay, M.D., & Helou, G. 1990, ApJ, 362, 59
Braine, J., & Combes, F., A&A,264, 433
Condon, J.J. 1987, ApJS, 65, 485
Devereux, N.A., Kenney, J.P., & Young, J.S. 1992, 103, 784
García-Barreto, J.A., Dettmar, R.-J., Combes, F., Ge M., & Koribalski, B., 1991*a*, RevMexAA, 22, 197
García-Barreto, J.A., Downes, D., Combes, F., Gerin, Magri, C., Carrasco, L., & Cruz-Gonzalez, I. 199 A&A, 244, 257
Giogia, I.M., Gregorini, L., & Klein, U. 1982, A&A, 1 164
Harwit, M., & Pacini, F. 1975, ApJ, 200, L127
Hawarden, T.G., Mountain, C.M., Leggett, S.K., Puxley, P.J. 1986, MNRAS, 221, 41p.
Helou, G., Soifer, B.T., & Rowan-Robinson, M. 19 ApJ, 298, L7
Helou, G. 1986, ApJ, 311, L33
Huchtmeier, W.K., & Richter, O.G. 1989, A Gene Catalog of H I Observations of Galaxies, (New Yc Springer Verlag)
Hummel, E., Jörsäter, S., Lindblad, P.O., & Sandqvist 1987*a*, A&A, 172, 32
Hummel, E., van der Hulst, J.M., & Keel W.C. 198 A&A,172, 51
Hummel, E. et al. 1990, A&A, 236, 333
Infrared Astronomical Satellite *(IRAS)* Catalogue a Atlases: The Point Source Catalog 1988, NASA 1 1190, Washington, D.C.
Israel, F.P., & van der Hulst, J.M. 1983, AJ, 88, 1736
Keel, W.C. 1983, ApJS, 52, 229
Keel, W.C., Kennicutt, R.C., Hummel, E., & van Hulst, J.M. 1985, AJ, 90, 708
Kenney, J., & Young, J. 1989, ApJ, 344, 171
Kennicutt, R.C., & Kent, S.M. 1983, AJ, 88, 1094
Klein, U., & Emerson, D.T. 1981, A&A, 94, 29
Persson, C.J.L, & Helou, G. 1987, ApJ, 314, 513
Pogge, R.W. 1989, ApJS, 71, 433
Romanishin, W. 1990, A&A, 100, 373
Scoville, N.Z., & Young, J.S. 1983, ApJ, 265, 148
Thronson, A. Jr., Hunter, D.A. Telesco, C.M., Gre house, M., & Harper, D.A. 1988, ApJ, 334, 605
Tully, R.B. 1988, Nearby Galaxies Catalog, (Cambrid Cambridge University Press), 201
Xu, C., Klein, U., Meinert, D., Wielebinski, R., & H nes, R.F. 1992, A&A, 257, 47
Young, J.S., Schloerb, F.P., Kenney, J.D., & Lord, S 1986, ApJ, 304, 443

R. Carrillo and J.A. García Barreto: Instituto de Astronomía, UNAM, Apartado Postal 70-264, 04510 Méxi D.F., México.
M. Dahlem: Hamburger Sternwarte, Gojenbergsweg 112, D2050 Hamburg 80, Germany.
U. Klein: Radio Astronomisches Institut der Universitaet Bonn, Auf dem Hügel 71, D-5300 Bonn Germany.